Topological Point Defects in Relaxor Ferroelectrics

Y. Nahas,[1,*] S. Prokhorenko,[1] I. Kornev,[2] and L. Bellaiche[1]
[1]Physics Department and Institute for Nanoscience and Engineering, University of Arkansas, Fayetteville, Arkansas 72701, USA
[2]Laboratoire Structures, Propriétés et Modélisation des Solides, CNRS-UMR8580, Ecole Centrale Paris, 92290 Châtenay-Malabry, France

(Received 22 July 2015; revised manuscript received 10 November 2015; published 24 March 2016)

First-principles-based effective Hamiltonian simulations are used to reveal the hidden connection between topological defects (hedgehogs and antihedgehogs) and relaxor behavior. Such defects are discovered to predominantly lie at the border of polar nanoregions in both $Ba(Zr_{0.5}Ti_{0.5})O_3$ (BZT) and $Pb(Sc_{0.5}Nb_{0.5})O_3$ (PSN) systems, and the temperature dependency of their density allows us to distinguish between noncanonical (PSN) and canonical (BZT) relaxor behaviors (via the presence or absence of a crossing of a percolation threshold). This density also possesses an inflection point at precisely the temperature for which the dielectric response peaks. Moreover, hedgehogs and antihedgehogs are found to be mobile excitations, and the dynamical nature of their annihilation is demonstrated (using simple hydrodynamical arguments) to follows laws, such as those of Vogel-Fulcher and Arrhenius, that are characteristic of dipolar relaxation kinetics of relaxor ferroelectrics.

DOI: 10.1103/PhysRevLett.116.127601

Relaxor materials form a class of disordered ferroelectrics embodying an intriguing case of the effect of quenched randomness on physical properties. A primary feature at the origin of their anomalous and technologically prominent properties is the emergence of inhomogeneous local order, and especially intriguing is its ensuing complex relaxation process [1–5]. It is commonly accepted that the confinement of polar order to within randomly oriented nanoregions is the result of the interplay between compositional disorder and the underlying ferroelectric phase instability [2,3]. Deviations from mean-field expectations have been associated with the onset of an ergodic relaxor state below T_d, the so-called Burns temperature where local order first nucleates [6]. On cooling, as the correlation length for dipolar fluctuations increases, polar regions grow in size, and depending on the kinetics of their development [7], ultimately show either canonical or noncanonical behavior [2,3]. In noncanonical relaxors such as $Pb(Sc_{0.5}Nb_{0.5})O_3$ (PSN) [7–9], polar regions percolate the whole sample and yield a static, cooperative relaxor-to-ferroelectric spontaneous phase transition at the Curie temperature, T_C, while in canonical relaxors such as $Ba(Zr_{0.5}Ti_{0.5})O_3$ (BZT) [10], they exhibit a dynamic slowing-down of their fluctuations that frustrates and impedes the development of long-range order. The dielectric relaxation (prior to the spontaneous phase transition in the case of PSN) characterizes the relaxor behavior. Moreover, in the relaxor state, the system has an average cubic symmetry. Interestingly, due to its wide applicability to many relaxational phenomena exhibiting cooperative behavior [2,11], the so-called Vogel-Fulcher relation [12,13] is often empirically used to analyze relaxation kinetics in relaxors [2,3,11], although no microscopic prescription has been firmly established for such a relation. It is given by

$$\tau = \tau_\infty \exp[U/k(T - T_0)], \tag{1}$$

where the reference temperature T_0 can be interpreted as the dipolar freezing temperature for the relaxation process, and can be viewed as defining a transition from an ergodic relaxor state to a nonergodic state [2].

In spite of abundant experimental investigations and numerous theoretical formulations [14–21], the subject of the relaxor behavior remains nonexhausted. In particular, a criterion for discerning between canonical and noncanonical behaviors is still lacking. One may also wonder whether a connection (though presently unknown) between relaxor behavior and topological defects [22,23] exists, especially when realizing that some models proposed to explain relaxor behavior are based on the existence of locally ordered polar nanoregions embedded within a disordered matrix [2,3], while point topological defects are known to occur wherever the order changes discontinuously [24], thereby concentrating distortions and enabling the surrounding medium to be locally ordered. Intuitively, invoking a topological analysis for relaxor behavior therefore rests upon the characteristic inhomogeneous local order. Since polar regions can locally adopt different low-symmetry polar states, wherever incompatible choices of symmetry breaking arise singularities in the dipolar order parameter vector field [22] can be expected to spontaneously form, therefore resulting in the creation of topological defects.

Finding such a hypothetical connection between relaxors and topological defects will be of significant importance since, owing to their ubiquitous nature, topological entities such as hedgehogs (point defects in three dimensions) and vortices (point defects in two dimensions) are now widely recognized as constituting a major topic in several different

areas of physics, including ferroelectrics [25]. They have been studied and experimentally observed in various systems, ranging from cosmology [26–28] to liquid crystals [29], and they often reveal a common logic among seemingly unrelated systems and offer the possibility of dually recasting the systems' (thermo)dynamics in formulations solely based on discrete sets of topological charges [30]. They are often expected to form spontaneously in proximity to many different types of phase transitions [31,32] and have been of crucial relevance for understanding otherwise dormant and unexplored properties such as those featured in superfluids, superconductors, liquid crystal, and crystals. Indeed, many features of these systems, such as plastic deformation of solids, the Kosterlitz-Thouless transition of the two-dimensional XY model [33], the dislocation-unbinding melting of solids [34], and the formation of colloidal crystals in nematic liquid crystals, to cite but a few, are dictated by their defects rather than by the properties of most of their bulk. Adding relaxor ferroelectrics to that list of materials thus stands as an exciting possibility.

In this Letter, we thus seek to isolate and exploit point topological defects [22,23] in view of examining whether such features correlate to the relaxor behavior, and whether they shed new light on relaxors. We numerically access the temperature evolution of the density ρ of topological point singularities (hedgehogs and antihedgehogs) for BZT and PSN, and identify the percolation threshold p_c of defects as a criterion for discriminating between canonical (BZT) and noncanonical (PSN) relaxor behaviors. Furthermore, evidence of the dynamical nature of topological defects enables us to make use of a hydrodynamic description involving a two-species diffusion-annihilation process among hedgehogs and antihedgehogs; this yields, in turn, the characteristic relaxation kinetics laws of relaxors.

Here, using first-principles-based effective Hamiltonians [35–37], we numerically investigate the behavior of hedgehogs and antihedgehogs in BZT and PSN relaxor ferroelectrics (see Supplemental Material [38] for a description of the effective Hamiltonian methodological framework). We consider random distribution of B-site cations for both systems and perform Monte Carlo simulations on $12 \times 12 \times 12$ and $18 \times 18 \times 18$ periodic supercells for $Ba(Zr_{0.5}Ti_{0.5})O_3$ and $Pb(Sc_{0.5}Nb_{0.5})O_3$, respectively, using at least 2×10^5 thermalization sweeps (note that PSN exhibits much stronger random fields than BZT [35,36] and that modeling such fields well requires the use of larger supercells). The calculations begin at high temperature from a cold start, and the temperature is then decreased in small steps to get well-converged results. We note that while the effective Hamiltonian employed to simulate the properties of BZT [35] yields characteristic temperatures in concordance with those experimentally reported (e.g., it gives a Burns temperature of $T_d \sim 450$ K, agreeing with the measured value given in Ref. [10]), the one used to simulate the properties of PSN overestimates characteristic temperatures (it yields a maximum of the static dielectric response occurring at the temperature $T_m \sim 950$ K while the reported experimental value is of 380 K [7]). Such discrepancy arises from the fact that the effective Hamiltonian of PSN [36,37] does not incorporate oxygen octahedral tiltings as degrees of freedom, which compete against the formation of electrical dipoles (via a repulsive biquadratic energy coupling these tiltings and dipoles [47]). We thus decided to rescale the temperature by substracting 570 K for PSN. We also follow Refs. [48–50] in order to assign a topological charge Q within each of the unit cells composing the supercell. Within this procedure, Q is guaranteed to be an integer and the net topological charge (that is, the sum of the topological charges within the supercell) is ensured to be zero as the considered systems are defined with periodic boundary conditions. We numerically found that the magnitude of the nonzero topological charges present in the investigated systems is almost always equal to unity. A hedgehog carries a charge

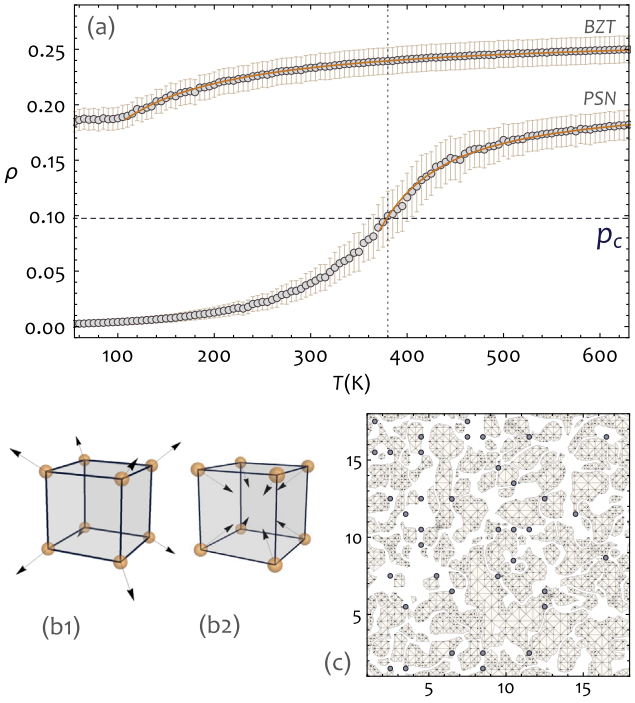

FIG. 1. (a) Temperature evolution of the density ρ of point topological defects (averaged over Monte Carlo sweeps) for BZT and PSN. Solid lines correspond to exponential fits in the relaxor range. Horizontal dashed line indicates the site percolation threshold p_c. Vertical dashed line indicates the temperature at which the p_c line intersects the defect density of PSN (~380 K). (b) Schematic illustration of point topological defects at atomic scale. Yellow spheres correspond to B-sites to which local dipole moments (arrows) are allocated. The enclosed defect in the unit cell is (b1) a hedgehog corresponding to a sourcelike dipolar pattern or (b2) an antihedgehog corresponding to a sinklike dipolar pattern. (c) Transverse cross sectional view of PSN supercell for $T = 430$ K showing the polar clusters (hatched regions) and the location of defects (circles) projected on the plane.

$Q = +1$ [Fig. 1(b1)] while an antihedgehog carries the opposite charge, $Q = -1$ [Fig. 1(b2)].

Let us now define the density ρ of topological defects as the ratio of topologically defective cells (i.e., containing hedgehogs or antihedgehogs) to the supercell volume. Figure 1(a) shows the evolution of the thermal average of ρ with temperature in both BZT and PSN. Moreover, and in order to relate ρ to (macroscopic and microscopic) properties of these two relaxor ferroelectrics, Fig. 2 reports the temperature derivative $d\rho/dT$ of the defect density along with the average diagonal component of the dielectric susceptibility tensor $\chi = (\chi_{11} + \chi_{22} + \chi_{33})/3$, as a function of temperature in both BZT and PSN. This latter tensor is practically calculated as in Refs. [35,51,52].

Figure 2 also displays the evolution with temperature of the Edwards-Anderson-like parameter q_{EA}, which is computed as $q_{\mathrm{EA}} = \langle \langle \mathbf{u}_i \rangle_s^2 \rangle_i$, where the inner averaging is performed on the s Monte Carlo sweeps while the outer one is made over the i lattice sites [35]. It also shows the temperature dependency of the specific heat C, which is extracted from the supercell energy fluctuations, $k_B T^2 C = \langle E^2 \rangle - \langle E \rangle^2$, where $\langle E \rangle$ corresponds to the average over Monte Carlo sweeps of the internal energy E and $\langle E^2 \rangle$ to that of its square, and where k_B is the Boltzmann constant. In case of BZT, q_{EA} is found to increase with decreasing temperature, thereby indicating the development of local correlations and the establishment of a glassy order upon cooling, in concordance with the experimentally reported dipolar glass character of BZT [53], for which no macroscopic order parameter (e.g., spontaneous polarization) exists down to the lowest temperature. On the other hand, the lower panel of Fig. 2 shows that PSN becomes ferroelectric, and thus loses its relaxor behavior below a certain finite temperature, since its specific heat exhibits a noticeable peak (the temperature at which C peaks is known to be the Curie temperature, T_C). The corresponding results reveal that $T_C \sim 360$ K, while the maximum of the static dielectric response χ occurs at a higher temperature $T_m \sim 380$ K in PSN, both in good agreement with experimental values [8].

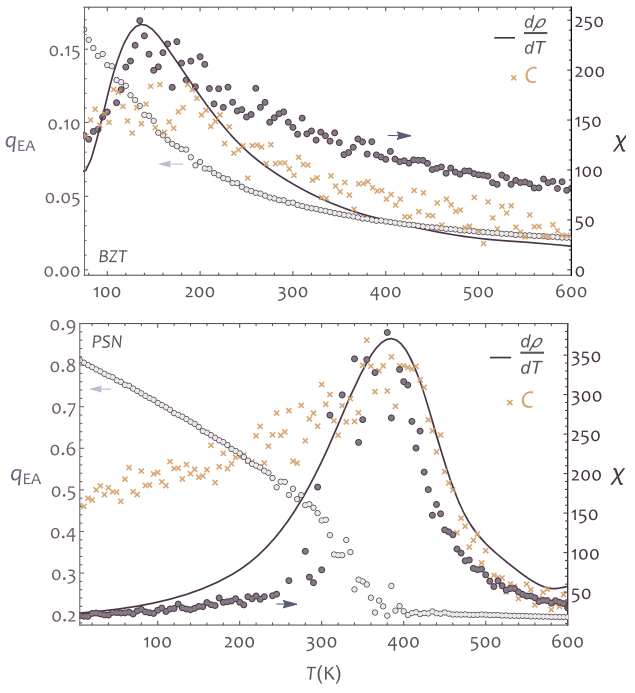

FIG. 2. Evolution with temperature of the Edwards-Anderson parameter q_{EA} (in arbitrary units), the specific heat C (in arbitrary units), one third of the trace of the dielectric susceptibility tensor χ (10^2), and the derivative $d\rho/dT$ of the defect density for BZT (upper panel) and PSN (lower panel).

Figure 1(a) indicates that, in case of BZT, the density ρ is found to decrease smoothly with decreasing temperature, and is nonzero over the entire temperature range. Moreover the upper panel of Fig. 2 reveals that the temperature at which this density of topological defects inflects (that is, the temperature at which $d\rho/dT$ is maximal) is ~135 K in BZT, which is precisely the temperature T_m at which its dielectric response χ peaks [10]. The lower panel of Fig. 2 confirms the identity between the inflection of ρ and the T_m temperature at which χ is maximal in PSN (which is about 380 K in this system, that is, about 20 K larger than its Curie temperature). These observations in both BZT and PSN therefore enable the interpretation of the defect density inflection point as the temperature at which the dielectric anomaly occurs in relaxor ferroelectrics. The connection between topological defects and relaxor properties takes its root into the fact that, as shown in Fig. 1(c), the spatial distribution of defects is such that they are mostly positioned at the contact points between rugged interfaces of differently ordered polar nanoregions (numerically identified using the procedure of Ref. [54]), that is, at the border of the objects believed to be responsible for relaxor behavior [2], where local distortions of the polarization vector field are at their utmost. For instance, we find that for PSN at 430 K the fraction of the topological defects that reside at the interfaces of polar nanoregions is of ~89%. Interestingly, such point topological defects are inherently associated with elastic deformations of cubic symmetry [as one can guess from Fig. 1(b) and from the known coupling between local dipoles and local strains], which may explain the experimentally reported diffuse scattering anisotropy [55].

Figure 1(a) further shows that, in contrast with BZT, ρ of PSN significantly drops around T_m, and ultimately vanishes for lower temperatures. It is particularly striking to realize that, in PSN, this T_m temperature coincides with the intersection between the defect density ρ and the percolation threshold p_c (shown by the horizontal dashed line in Fig. 1). More precisely, p_c indicates the site percolation threshold on a regular lattice with neighborhood extending to the third-nearest neighbors [56], and corresponds to the critical probability above which a cluster of topological

defects spanning through the whole system appears. This suggests that in the temperature region where $\rho > p_c$, the development of long-range order is hindered by percolating clusters of topological defects, while for $\rho < p_c$, the density is such that long-range ferroelectric order is achievable. In this regard, ρ dually provides information about the evolution of local order. As a matter of fact, in both PSN and BZT, the gradual lessening of hedgehogs and antihedgehogs with decreasing temperature indicates the growth of polar regions. On further cooling, in the case of canonical BZT, ρ retains a value larger than p_c, thereby indicating the impeded expansion of polar regions. Persisting hedgehogs and antihedgehogs prohibit the establishment of long-range order at any finite temperature, and the average crystal symmetry remains cubic in BZT. In the case of noncanonical PSN, on cooling below T_m, ρ drops beneath p_c, thereby signaling that enhanced dipolar correlations effectively cancel the influence of internal random fields and induce long-range ferroelectric order. These observations, hence, point to a topological-based criterion for distinguishing between canonical and noncanonical relaxor behaviors, via the presence or absence, respectively, of a crossing of p_c by ρ. Note that we further tested this criterion of the appearance of ferroelectricity when ρ equals p_c on a prototypical ferroelectric, $Pb(Zr_{0.6}Ti_{0.4})O_3$ (see Supplemental Material [38]).

Interestingly, since the total topological charge is constrained to be zero in systems with periodic boundaries conditions, the decrease of ρ occurring upon cooling in both BZT and PSN can only happen by annihilation among defects of opposite topological charge, that is, between hedgehogs (Q_+) and antihedgehogs (Q_-). It is thus of interest to inquire into the dynamical nature of topological singularities and their annihilation (note that the Supplemental Material [38] provides a Monte Carlo time autocorrelation analysis of defects spatial distribution). For that, we make use of a hydrodynamic description involving a two-species diffusion-annihilation process, $Q_+ + Q_- \rightarrow \emptyset$, with long-range forces [57,58]. Therein, the account for conserved charge density fluctuations and a power-law long-range interaction, usually of a Coulomb type, among charged particles leads to an attraction between annihilating partners and entails a new mechanism for slow dynamics [57,58]. The annihilation behavior for a Coulombic system in two dimensions has been of widespread interest because of its connection with XY-model kinetics [59], in which vortices and antivortices interact via $(1/r)$ force and exhibit nontrivial dynamics. Such processes have also been studied in liquid-crystal physics, where the singularities of the smectic director field appear as positive and negative vortices interacting via a logarithmic potential due to elastic forces [60,61]. In three dimensions, it is expected that, in the presence of a Coulomb interaction, the relaxation time τ of such processes is inversely proportional to the density ρ [57,58]. Coming back to the dependence of ρ on temperature (Fig. 1), we find that for $T > T_0$, the density ρ of PSN can be very well approximated by an exponential relation [62] $\rho_0 + (\rho_\infty - \rho_0)\exp[-w/(T - T_0)]$, where T_0 is found to coincide with T_C. Since the fitted values give ratios of ρ_∞ to ρ_0 that is much greater than 1 ($\sim$28), one thus obtains a relaxation time associated with the annihilation process between hedgehogs and antihedgehogs that is given by $\tau \propto (\rho_\infty - \rho_0)^{-1}\exp[w/(T - T_0)]$. Remarkably, this latter equation has precisely the analytical form of the Vogel-Fulcher relaxation law that is a typical characteristic of dipolar relaxation in relaxor ferroelectrics, including PSN [Eq. (1)]. Notably, it was reported for PSN that the ferroelectric phase transition coincides with the freezing temperature T_f [63], thus enabling the identification $T_0 \sim T_f \sim T_C$. We find that the parameter w entering the fit of ρ of PSN by $\rho_0 + (\rho_\infty - \rho_0)\exp[-w/(T - T_0)]$ is $\sim$41 K (0.0035 eV), that is, about one order of magnitude lower than that reported for dipolar relaxation measurements [8]. Moreover, in the case of BZT, the density can be well fitted by $\rho_\infty \exp[-w/T]$, but only for temperatures above $\sim$108 K, yielding instead an Arrhenius law for τ rather than a Vogel-Fulcher relation. Interestingly, a thermally activated Arrhenius relaxation, as well as a departure from it below a certain temperature, have already been pointed out for BZT for the (low) frequency associated with the relaxation of electric dipoles [53,64]. The parameter w appearing in the fit of ρ by $\rho_\infty \exp[-w/T]$ is about $\sim$38 K (0.0032 eV) in BZT, which is, as in the case of PSN, also about one order of magnitude lower than that associated with the reported dipolar relaxation of BZT [64]. One can therefore conclude that the annihilation process between hedgehogs and antihedgehogs follows the same type of law as dipolar relaxation (namely, Vogel-Fulcher in PSN versus Arrhenius in BZT), but with activation energy being smaller by one order of magnitude. The latter numerically obtained values of w are to be associated with the lifetime of defect pairs fluctuations [31,65] rather than with the average energy barrier between different orientations of individual dipoles within polar nanoregions [11]. It is worth noting that topological defects have structures that are stable against small fluctuations of the polarization vector field. Interestingly, this topological stability can lead to important effects on the dynamics of the system, preventing the rapid relaxation of such local distortions and endowing defects with long lifetimes and slow dynamics [66,67].

Furthermore, from the point of view of topological defects, the obtained Arrhenius relation for the temperature dependence of the relaxation time in BZT can be ascribed to screened interactions among topological defects. Indeed, Fig. 1(a) shows that, unlike PSN, BZT retains a high defect density down to the lowest temperatures (around 18% of the volume of the supercell is defective), and the defect-mediated relaxation can be seen as effectively involving noninteracting point singularities. For $T < 108$ K, we find

that continued loss of the defects' mobility, or conversely, increased memory effects (see Supplemental Material [38]) concomitantly occurs with a stagnation of their density [a plateau is reached by ρ of BZT, Fig. 1(a)]. Interestingly, the residual relaxation rate at very low temperatures (see Supplemental Material [38]) hints to a large density of states for topological excitations at the lowest energies, which is a signature of frustration and glassiness [68].

In summary, by adopting a topological approach for probing the relaxor behavior, we have identified the percolation of topological disorder as a criterion for discerning between canonical and noncanonical relaxor behaviors. We also found that the dielectric anomaly occurs at the temperature at which the density of defects inflects. Moreover, making use of a simple hydrodynamic description involving diffusion-annihilation process among Coulombically interacting oppositely charged topological defects, we found that the dynamics of defects relates to that of relaxors within a defect-mediated relaxation mechanism.

This work is supported by the ARO Grant No. W911NF-12-1-0085. S. P. and L. B. are also thankful for the financial support of DARPA Grant No. HR0011-15-2-0038 (MATRIX program).

*yousra.nahas@gmail.com

[1] G. A. Smolenskii and A. I. Agranovskaya, Sov. Phys. Solid State **1**, 1429 (1960).
[2] G. A. Samara, Solid State Phys. **56**, 239 (2001).
[3] A. A. Bokov and Z. G. Ye, J. Mater. Sci. **41**, 31 (2006).
[4] W. Kleemann, J. Adv. Dielect. **02**, 1241001 (2012).
[5] G. H. Haertling and C. E. Land, J. Am. Ceram. Soc. **54**, 303 (1971); G. H. Haertling, Ferroelectrics **75**, 25 (1987).
[6] G. Burns and F. H. Dacol, Phys. Rev. B **28**, 2527 (1983).
[7] Y. H. Bing, A. A. Bokov, and Z. G. Ye, Curr. Appl. Phys. **11**, S14 (2011).
[8] F. Chu, I. M. Reaney, and N. Setter, J. Appl. Phys. **77**, 1671 (1995).
[9] C. Malibert, B. Dkhil, J. M. Kiat, D. Durand, J. F. Berar, and A. Spasojevic-de Bire, J. Phys. Condens. Matter **9**, 7485 (1997).
[10] T. Maiti, R. Gu, and A. S. Bhalla, J. Am. Ceram. Soc. **91**, 1769 (2008).
[11] G. A. Samara, Ferroelectrics **117**, 347 (1991), and references therein.
[12] H. Vogel, Phys. Z. **22**, 645 (1921).
[13] G. S. Fulcher, J. Am. Ceram. Soc. **8**, 339 (1925).
[14] L. E. Cross, Ferroelectrics **76**, 241 (1987).
[15] B. E. Vugmeister and H. Rabitz, Phys. Rev. B **57**, 7581 (1998).
[16] V. Westphal, W. Kleemann, and M. D. Glinchuk, Phys. Rev. Lett. **68**, 847 (1992).
[17] R. Blinc, J. Dolinsek, A. Gregorovic, B. Zalar, C. Filipic, Z. Kutnjak, A. Levstik, and R. Pirc, Phys. Rev. Lett. **83**, 424 (1999); R. Pirc and R. Blinc, Phys. Rev. B **60**, 13470 (1999).
[18] V. V. Kirillov and V. A. Isupov, Ferroelectrics **5**, 3 (1973).
[19] V. A. Stephanovich, Eur. Phys. J. B **18**, 17 (2000).
[20] A. P. Levanyuk and R. Blinc, Phys. Rev. Lett. **111**, 097601 (2013).
[21] Y. Nahas and I. Kornev, Europhys. Lett. **103**, 37013 (2013).
[22] N. D. Mermin, Rev. Mod. Phys. **51**, 591 (1979).
[23] J. Vannimenus, in *Polymers, Liquid Crystals, and Low-Dimensional Solids* (Springer, New York, 1985), p. 567.
[24] B. G. Chen, G. P. Alexander, and R. D. Kamien, Proc. Natl. Acad. Sci. U.S.A. **106**, 15577 (2009).
[25] S. E. Rowley and G. G. Lonzarich, Nat. Phys. **10**, 907 (2014).
[26] T. W. B. Kibble, J. Phys. A **9**, 1387 (1976).
[27] W. H. Zurek, Nature (London) **317**, 505 (1985).
[28] W. H. Zurek, Phys. Rev. Lett. **102**, 105702 (2009).
[29] G. Toth, C. Denniston, and J. M. Yeomans, Phys. Rev. Lett. **88**, 105504 (2002).
[30] S. Z. Lin, Nat. Phys. **10**, 970 (2014).
[31] M. H. Lau and C. Dasgupta, Phys. Rev. B **39**, 7212 (1989).
[32] C. Holm and W. Janke, J. Phys. A **27**, 2553 (1994).
[33] J. M. Kosterlitz and D. J. Thouless, J. Phys. C **6**, 1181 (1973).
[34] B. I. Halperin and D. R. Nelson, Phys. Rev. Lett. **41**, 121 (1978).
[35] A. R. Akbarzadeh, S. Prosandeev, E. J. Walter, A. Al-Barakaty, and L. Bellaiche, Phys. Rev. Lett. **108**, 257601 (2012).
[36] J. Iniguez and L. Bellaiche, Phys. Rev. B **73**, 144109 (2006).
[37] R. Hemphill, L. Bellaiche, A. Garcia, and D. Vanderbilt, Appl. Phys. Lett. **77**, 3642 (2000).
[38] See Supplemental Material at http://link.aps.org/supplemental/10.1103/PhysRevLett.116.127601, which includes Refs. [39–46], for additional methodological information, results for $Pb(Zr_{0.6}Ti_{0.4})O_3$ prototypical ferroelectric, and Monte Carlo time autocorrelation analysis of defects' spatial distribution.
[39] W. Zhong, D. Vanderbilt, and K. M. Rabe, Phys. Rev. Lett. **73**, 1861 (1994).
[40] W. Zhong, D. Vanderbilt, and K. M. Rabe, Phys. Rev. B **52**, 6301 (1995).
[41] L. Bellaiche and D. Vanderbilt, Phys. Rev. B **61**, 7877 (2000).
[42] N. J. Ramer and A. M. Rappe, J. Phys. Chem. Solids **61**, 315 (2000).
[43] L. Bellaiche, A. Garcia, and D. Vanderbilt, Ferroelectrics **266**, 41 (2002).
[44] L. Bellaiche, A. Garcia, and D. Vanderbilt, Phys. Rev. Lett. **84**, 5427 (2000).
[45] H. E. A. Huitema and J. P. van der Eerden, J. Chem. Phys. **110**, 3267 (1999).
[46] B. Dkhil, P. Gemeiner, A. Al-Barakaty, L. Bellaiche, E. Dulkin, E. Mojaev, and M. Roth, Phys. Rev. B **80**, 064103 (2009).
[47] I. A. Kornev, L. Bellaiche, P.-E. Janolin, B. Dkhil, and E. Suard, Phys. Rev. Lett. **97**, 157601 (2006).
[48] O. I. Motrunich and A. Vishwanath, Phys. Rev. B **70**, 075104 (2004).
[49] S. Sachdev and K. Park, Ann. Phys. (Amsterdam) **298**, 58 (2002).
[50] B. Berg and M. Luscher, Nucl. Phys. **B190**, 412 (1981).
[51] A. Garcia and D. Vanderbilt, in *First-Principles Calculations For Ferroelectrics: Fifth Williamsburg Workshop*, edited by R. E. Cohen (AIP, Woodbury, NY, 1998), p. 53.

[52] K. M. Rabe and E. Cokayne, in *First-Principles Calculations for Ferroelectrics: Fifth Williamsburg Workshop*, edited by R. E. Cohen (AIP, Woodbury, NY, 1998), p. 61.
[53] J. Petzelt, D. Nuzhnyy, M. Savinov, V. Bovtun, M. Kempa, T. Ostapchuk, J. Hlinka, G. Canu, and V. Buscaglia, Ferroelectrics **469**, 14 (2014).
[54] Y. Nahas, Ph.D. thesis, Ecole Centrale Paris, 2013.
[55] R. G. Burkovsky, A. V. Filimonov, A. I. Rudskoy, K. Hirota, M. Matsuura, and S. B. Vakhrushev, Phys. Rev. B **85**, 094108 (2012).
[56] L. Kurzawski and K. Malarz, Rep. Math. Phys. **70**, 163 (2012).
[57] V. V. Ginzburg, P. D. Beale, and N. A. Clark, Phys. Rev. E **52**, 2583 (1995).
[58] V. V. Ginzburg, L. Radzihovsky, and N. A. Clark, Phys. Rev. E **55**, 395 (1997).
[59] R. Loft and T. A. DeGrand, Phys. Rev. B **35**, 8528 (1987).
[60] R. Pindak, C. Y. Young, R. B. Meyer, and N. A. Clark, Phys. Rev. Lett. **45**, 1193 (1980).
[61] C. D. Muzny and N. A. Clark, Phys. Rev. Lett. **68**, 804 (1992).
[62] N. D. Antunes, L. M. A. Bettencourt, and M. Kunz, Phys. Rev. E **65**, 066117 (2002).
[63] F. Chu, I. M. Reaney, and N. Setter, Ferroelectrics **151**, 343 (1994).
[64] D. Wang, J. Hlinka, A. A. Bokov, Z. G. Ye, P. Ondrejkovic, J. Petzelt, and L. Bellaiche, Nat. Commun. **5**, 5100 (2014).
[65] J. Tobochnik and G. V. Chester, Phys. Rev. B **20**, 3761 (1979).
[66] J. Vannimenus, in *Topological Defects and Disordered Systems* (Springer, New York, 1984), pp. 567–616.
[67] A. P. Balachandran and S. Digal, Int. J. Mod. Phys. A **17**, 1149 (2002).
[68] S. R. Dunsiger, R. F. Kiefl, K. H. Chow, B. D. Gaulin, M. J. P. Gingras, J. E. Greedan, A. Keren, K. Kojima, G. M. Luke, W. A. MacFarlane, N. P. Raju, J. E. Sonier, Y. J. Uemura, and W. D. Wu, Phys. Rev. B **54**, 9019 (1996).